AMERICAN SOCIETY FOR MICROBIOLOGY | mBio

Antimicrobial Chemotherapy | Research Article

OXA β-lactamases from *Acinetobacter* spp. are membrane bound and secreted into outer membrane vesicles

Lucia Capodimonte,[1,2] Fernando Teixeira Pinto Meireles,[3] Guillermo Bahr,[1,2] Robert A. Bonomo,[4,5,6,7] Matteo Dal Peraro,[3] Carolina López,[1] Alejandro J. Vila[1,2,7]

AUTHOR AFFILIATIONS See affiliation list on p. 15.

ABSTRACT β-lactamases from Gram-negative bacteria are generally regarded as soluble, periplasmic enzymes. NDMs have been exceptionally characterized as lipoproteins anchored to the outer membrane. A bioinformatics study on all sequenced β-lactamases was performed that revealed a predominance of putative lipidated enzymes in the Class D OXAs. Namely, 60% of the OXA Class D enzymes contain a lipobox sequence in their signal peptide, that is expected to trigger lipidation and membrane anchoring. This contrasts with β-lactamases from other classes, which are predicted to be mostly soluble proteins. Almost all (>99%) putative lipidated OXAs are present in *Acinetobacter* spp. Importantly, we further demonstrate that OXA-23 and OXA-24/40 are lipidated, membrane-bound proteins in *Acinetobacter baumannii*. In contrast, OXA-48 (commonly produced by Enterobacterales) lacks a lipobox and is a soluble protein. Outer membrane vesicles (OMVs) from *A. baumannii* cells expressing OXA-23 and OXA-24/40 contain these enzymes in their active form. Moreover, OXA-loaded OMVs were able to protect *A. baumannii*, *Escherichia coli*, and *Pseudomonas aeruginosa* cells susceptible to piperacillin and imipenem. These results permit us to conclude that membrane binding is a bacterial host-specific phenomenon in OXA enzymes. These findings reveal that membrane-bound β-lactamases are more common than expected and support the hypothesis that OMVs loaded with lipidated β-lactamases are vehicles for antimicrobial resistance and its dissemination. This advantage could be crucial in polymicrobial infections, in which *Acinetobacter* spp. are usually involved, and underscore the relevance of identifying the cellular localization of lactamases to better understand their physiology and target them.

IMPORTANCE β-lactamases represent the main mechanism of antimicrobial resistance in Gram-negative pathogens. Their catalytic function (cleaving β-lactam antibiotics) occurs in the bacterial periplasm, where they are commonly reported as soluble proteins. A bioinformatic analysis reveals a significant number of putative lipidated β-lactamases, expected to be attached to the outer bacterial membrane. Notably, 60% of Class D OXA β-lactamases (all from *Acinetobacter* spp.) are predicted as membrane-anchored proteins. We demonstrate that two clinically relevant carbapenemases, OXA-23 and OXA-24/40, are membrane-bound proteins in *A. baumannii*. This cellular localization favors the secretion of these enzymes into outer membrane vesicles that transport them outside the boundaries of the cell. β-lactamase-loaded vesicles can protect populations of antibiotic-susceptible bacteria, enabling them to thrive in the presence of β-lactam antibiotics. The ubiquity of this phenomenon suggests that it may have influenced the dissemination of resistance mediated by *Acinetobacter* spp., particularly in polymicrobial infections, being a potent evolutionary advantage.

KEYWORDS lipidated β-lactamases, OXA β-lactamases, *Acinetobacter* spp., outer membrane vesicles, dissemination of antimicrobial resistance

Editor Edward W. Yu, Case Western Reserve University School of Medicine, Cleveland, Ohio, USA

Address correspondence to Carolina López, lopez@ibr-conicet.gov.ar, or Alejandro J. Vila, vila@ibr-conicet.gov.ar.

The authors declare no conflict of interest.

See the funding table on p. 16.

Received 30 October 2024
Accepted 19 November 2024
Published 13 December 2024

Bacteria possess a potent and diverse arsenal to resist the action of antibiotics. Gram-negative bacteria have predominantly evolved the expression of β-lactamases as one of the main mechanisms of resistance against β-lactam antibiotics (1, 2). To date, more than 8,200 different β-lactamase variants are reported (3), a number that is increasing at an alarming pace. The evolution and dissemination of genes coding for β-lactamases in opportunistic and pathogenic bacteria has been accelerated by the misuse and overuse of antibiotics worldwide, representing a major challenge for public health (1, 4).

β-lactamases are classified into four groups (A, B, C, and D) according to the Ambler system, based on sequence homology (5). Class A, C, and D enzymes are serine-β-lactamases (SBLs), which share a common protein fold, but display differences in their active sites and catalytic mechanisms (6, 7). In contrast, Class B enzymes are metallo-β-lactamases (MBLs) requiring Zn (6) ions for their hydrolytic activity (8). From the clinical point of view, carbapenemases are the largest public health threat since they are able to inactivate carbapenems, the most potent β-lactams available in clinical practice (9, 10). Carbapenemases have been identified in three out of these four classes, including all Class B MBLs, members of Class A (KPC, GES, and NMC) and many Class D β-lactamases (from the OXA family, named upon their oxacillinase activity) (11, 12).

In Gram-negative bacteria, mature β-lactamase enzymes are localized in the periplasmic space (13–16), where they cleave β-lactam antibiotics, thwarting their activity against enzymes involved in peptidoglycan cross-linking. β-lactamases have been historically regarded as soluble periplasmic enzymes. In contrast, a reduced number of β-lactamases have been exceptionally characterized as lipoproteins anchored to the inner leaflet of the outer membrane, such as the Class A enzymes BRO-1 from *Moraxella catarrhalis* (17) and PenI from *Burkholderia pseudomallei* (18). More recently, the widespread Zn-dependent carbapenemase NDM (6) (with 68 reported clinical variants to date) was identified as a lipidated, membrane-bound enzyme, a localization that enhances the stability of this enzyme upon the zinc starvation process during an infection (19, 20).

β-lactamases are produced as cytoplasmic precursors with an N-terminal signal sequence (the signal peptide) that directs these precursors to one of the two main export pathways (Sec or Tat) responsible for protein translocation into the periplasmic space (13). Most biochemically characterized β-lactamases have been shown to translocate across the inner membrane via the Sec system (14, 16). In the case of soluble, non-lipidated β-lactamases, the type I signal peptidase (S cleaves the signal peptides of the precursor enzymes to generate the mature proteins (13, 21, 22). Instead, in the case of lipoproteins, the signal peptides are cleaved by the Type II signal peptidase (SpII) during the lipoprotein maturation process (16). Lipoprotein precursors possess a characteristic four amino acid motif known as a lipobox (23). The lipobox consensus sequence is [LVI]-[ASTVI]-[GAS]-C (24–26). The lipidation machinery in the periplasm transfers a diacylglycerol group to the free sulfhydryl of the cysteine residue in the lipobox and cleaves the signal sequence, leaving an acylated cysteine at the N-terminus. A further acyl group is then added generating a mature, triacylated lipoprotein that is inserted into the membrane (27). This lipidation mechanism has been thoroughly characterized in *E. coli* and it is widespread among Enterobacterales and non-fermenters (25, 28, 29).

In the case of NDM-1, membrane anchoring stabilizes this MBL against zinc deprivation and favors its incorporation into outer membrane vesicles (OMVs) (19). These nano-sized spherical structures bud and detach from the outer membrane of Gram-negative bacteria (30), playing several roles as decoys for phages and antibiotics, transporting nucleic acid, outer membrane, and periplasmic proteins as well as insoluble cargo (31, 32). Similar processes have also been reported in Gram-positive organisms (33). NDM incorporation into vesicles increases the available enzyme levels at the infection site, extending antibiotic hydrolysis beyond the limits of the bacterial cell (20). As a result, NDM-loaded vesicles can protect populations of otherwise antibiotic-susceptible

bacteria (19). Furthermore, vesicles can also mediate the transfer of the bla_{NDM-1} gene between bacteria (34, 35). The selection of the protein cargo in the case of NDM-1 depends on the interaction with the bacterial membrane, in which the covalent attachment through the lipid moiety is the main determinant (36, 37).

To explore the ubiquity of lipidation among β-lactamases, we performed a bioinformatic analysis of the signal peptides of all β-lactamases deposited in the β-lactamase database (www.BLDB.eu) (3). This study reveals a low number of lipobox sequences in enzymes from Classes A, B, and C. In contrast, almost 60% of Class D β-lactamases (most of them OXA enzymes) have a lipobox sequence and are thus predicted to be membrane-bound lipoproteins. Noteworthy, all putative OXA β-lactamase lipoproteins are found in *Acinetobacter* spp. Herein, we provide experimental evidence that the clinically relevant carbapenemases OXA-23 and OXA-24/40 from *A. baumannii* are membrane-bound lipoproteins. Disruption of the lipobox via mutagenesis results in the expression of soluble enzymes, supporting the bioinformatics analysis and molecular simulations.

The membrane-bound localization of OXA β-lactamases favors their incorporation into OMVs, as reported for NDM-1. The evolving hypothesis is that these OXA-loaded vesicles are capable of improving survival of not only *Acinetobacter* spp. in conditions of high β-lactam concentrations but also β-lactam-susceptible bacteria that are present in polymicrobial infections. We conclude that membrane-bound β-lactamases and their vesicle packaging represent a significant adaptation response in *Acinetobacter* spp. We propose that this cellular localization, linked to the secretion of lactamases into OMVs, represents an evolutionary advantage for *A. baumannii*, a highly troublesome pathogen associated with community-acquired and nosocomial infections. The protective effect of these vesicles confers a population advantage provided by *A. baumannii* OXA-producers in multiple clinical environments.

RESULTS

Bioinformatics predict that most Class D β-lactamases (OXAs) are lipidated

To identify putative lipidated β-lactamases, we performed an *in silico* analysis of all β-lactamase sequences available in the BLDB database (3) using the SignalP 6.0 server (38). This server employs a machine-learning algorithm that classifies signal peptides into one of the five known types (Sec/SPI, Sec/SPII, Sec/SPIII, Tat/SPI, and Tat/SPII) by means of a score that predicts the possibility of the signal peptide being transported and processed by each system. Our intention was to label all reported β-lactamases into soluble and lipidated enzymes. Despite the focus of the current work being on β-lactamases in Gram-negative organisms, the analysis covered all sequenced enzymes.

From a total number of 7,479 accessible β-lactamase sequences (April 2024), 7,226 were predicted to contain an N-terminal signal peptide targeting the Sec translocation pathway (97%) (Fig. 1A), confirming that most β-lactamases are Sec substrates (16). The small proportion of β-lactamases predicted to be translocated by the Tat system mostly belong to highly divergent Class A enzymes, suggesting that this feature does not imply any evolutionary connection among them but, instead, an adaptation to each organism. Indeed, there are enzymes from Gram-negative bacteria such as *Burkholderia* spp. (PenA and PenI enzymes), *Xanthomonas* spp. (XCC enzymes), and *Mycobacterium* spp. (MFO from *M. fortuitum* and MAB from *M. abscessus*) and from the Gram-positive organism *Streptomyces* spp. (SDA enzymes) (Table S1).

The identification of a lipobox sequence helps annotate proteins as substrates of the signal peptidase II, therefore targets for lipidation and membrane anchoring. Lipoboxes were identified in the sequences of 17% of Class A enzymes, 10% of Class B, and only twelve (0.3%) Class C β-lactamases (Fig. 1B; Table 1). This result agrees with the consensus that considers β-lactamases as soluble periplasmic proteins. In stark contrast, ca. 60% of Class D enzymes are putative lipoproteins (Fig. 1B; Table 2). Table 1 shows several representative Class A and B β-lactamases predicted as lipidated proteins, while Table 2 lists all families of putative lipidated OXAs. We also indicate the most likely

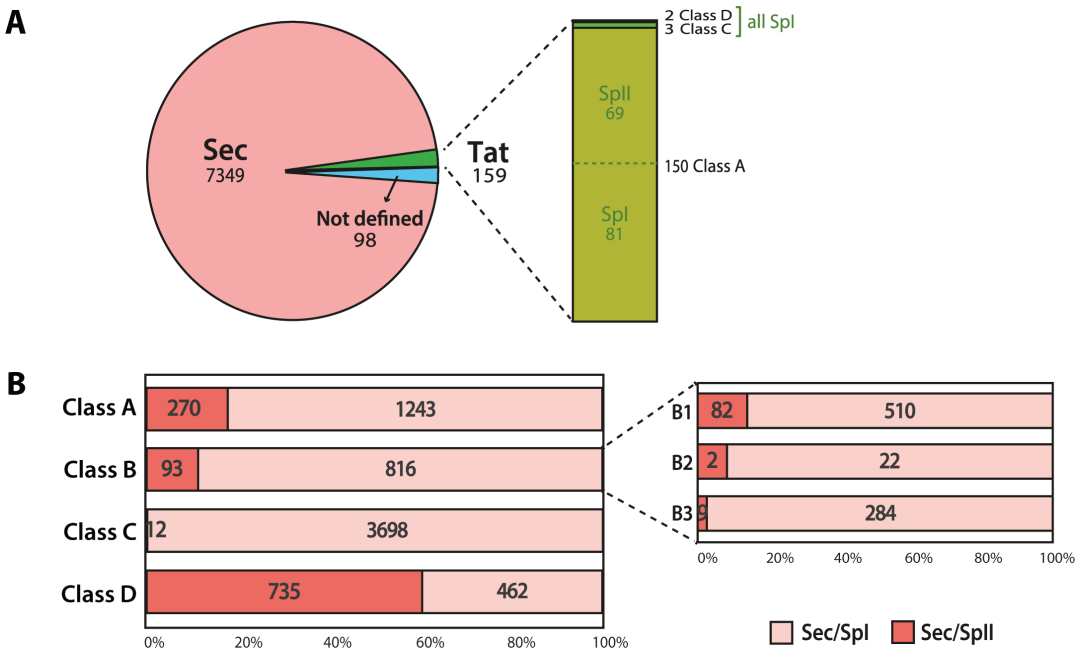

FIG 1 Class D contains the largest family of putative lipidated β-lactamases. (A) Pie chart indicating the number of β-lactamase sequences predicted to be translocated by the Sec and Tat systems. The bar at the right shows the distribution of β-lactamases translocated by the Tat system in each class, detailing if they are putative substrates of SpI (putative soluble proteins) or SpII (putative lipoproteins). (B) Putative substrates of SpI or SpII translocated by the Sec system, separated according to the β-lactamase class. The absolute numbers of each category are indicated inside each bar. The three subclasses of Class B enzymes (B1–B3) are indicated at the right. Class D enzymes show the largest number of predicted lipoproteins.

translocation and processing pathway in each case. Table S1 includes the predictions for all β-lactamases, with the scores provided by the SignalP 6.0 server.

The putative lipoproteins belonging to Class A include an important number of enzymes from Gram-positive and Gram-negative bacteria, a few of them already characterized experimentally. BcIII from *Bacillus cereus* was the first characterized membrane-bound lactamase (39). Later, BRO-1 was the first β-lactamase from a Gram-negative bacteria characterized as a membrane-bound protein (17). BRO-1 and BRO-2 from *M. catarrhalis*, are both predicted as lipoproteins dependent on the Tat

TABLE 1 β-lactamases from Classes A and B with lipoboxes in their signal peptides[a]

Ambler class or subclass	β-lactamase	Organism	Translocation system
A	BcIII*	*Bacillus cereus*	Sec/SpII
A	BlaC	*Mycobacterium tuberculosis*	Tat/SpII
A	BlaP-1/2	*Bacillus licheniformis*	Sec/SpII
A	BRO-1*/2*	*Moraxella catarrhalis*	Tat/SpII
A	PC-1*	*Staphylococcus aureus*	Sec/SpII
A	PenA-1/39	*Burkholderia multivorans*	Tat/SpII
A	PenI-1/8*	*Burkholderia pseudomallei*	Tat/SpII
A	ROB-1/5, 8/13	*Pasteurellales, Moraxella* spp.	Sec/SpII
B1	AFM-1/4	*Burkholderiales, Pseudomonas* spp.	Sec/SpII
B1	NDM-1/68*	Enterobacterales, non-fermenters	Sec/SpII
B3	ECM-1	*Erythrobacter citreus*	Sec/SpII
B3	EFM-1	*Erythrobacter flavus*	Sec/SpII
B3	EVM-1	*Erythrobacter vulgaris*	Sec/SpII

[a]The asterisk next to the lactamase names indicate the enzymes for which the membrane localization has been experimentally assessed. The most frequent organisms expressing the lactamase gene are indicated in the third column.

TABLE 2 Predicted cellular localization of principal Class D β-lactamases[a]

Class D β-lactamase	Number of enzymes	Organism(s)	Predicted cell localization
OXA-1-like	12	*Pseudomonadales, Shewanellaceae, Pasteurellales, Enterobacterales*	Soluble
OXA-2-like	31	*Pseudomonadales, Burkholderiales, Shewanellaceae, Enterobacterales, Vibrionales, Pasteurellales*	Soluble
OXA-10-like	60	*Burkholderiales, Pseudomonadales, Shewanellaceae, Enterobacterales*	Soluble
OXA-22-like	7	*Ralstonia* spp.	Soluble
OXA-23-like	49	*Acinetobacter* spp.[b]	Lipidated
OXA-24/40-like	24	*Acinetobacter* spp.	Lipidated
OXA-48-like	66	Enterobacterales, Shewanellaceae	Soluble
OXA-50-like	60	*Pseudomonas* spp.	Soluble
OXA-51-like	382	*Acinetobacter* spp.	Lipidated
OXA-58-like	8	*Acinetobacter* spp.	Lipidated
OXA-60-like	7	*Ralstonia* spp.	Soluble
OXA-134-like	34	*Acinetobacter* spp.	Lipidated
OXA-61-like	49	*Campylobacter* spp.	Soluble
OXA-211-like	17	*Acinetobacter* spp.	Lipidated
OXA-213-like	51	*Acinetobacter* spp.	Lipidated

[a]The Organism(s) column specifies the most reported organisms carrying the lactamase gene or the order to which they belong. The three OXA proteins selected in this study are shaded (OXA-23, 24/40, and 48, the representative members of each of these families). Table S2 describes all OXA subfamilies.
[b]OXA-73 and OXA-1095 sequences are deposited as plasmid and chromosomal genes of *Klebsiella pneumoniae*, respectively. No related articles available.

system. PenI enzyme from *B. pseudomallei* was experimentally shown to be a membrane-bound protein (18). Here, we show that the variants of PenA, PenB, PenI, and other members of the Pen family produced by *Burkholderia* species are predicted as lipoproteins translocated by the Tat system.

In the case of Class B MBLs, subclass B1 includes all variants of AFM and NDM enzymes, CHM-1, and ZOG-1, as putative lipoproteins dependent on the Sec system. No proteins from subclass B2 were predicted to be lipidated with a high score. However, within subclass B3, certain enzymes were identified as lipoproteins (Table 1).

Most Class D β-lactamases are also known as oxacillinase enzymes or OXAs (12). Remarkably, all putative lipidated OXAs are chromosomally encoded or acquired from *Acinetobacter* species, except for OXA-63-like enzymes from *Brachyspira pilosicoli*, OXA-347, -1089, and -1090 (26 out of 735 OXA enzymes). Indeed, the main groups of carbapenem-hydrolyzing Class D β-lactamases (CHDL) were predicted as lipoproteins: the chromosomally encoded OXA-51-like and the acquired OXA-23-like, OXA-58-like, and OXA-24/40-like (Table 2). In contrast, soluble OXA enzymes are not predicted in *Acinetobacter* species. This direct link between protein lipidation and a bacterial host (*Acinetobacter*, in this case) is unique to Class D enzymes, since lipidated Class A and B enzymes are found in a wide variety of bacterial hosts (Tables 1 and 2).

Molecular simulations reveal a mechanism for membrane association for lipidated OXA β-lactamases

To better characterize their possible association with membranes, we selected and performed coarse-grained molecular dynamics (CG-MD) simulations of the two most clinically important β-lactamases related to carbapenem resistance: OXA-23 and OXA-24/40. We ran the simulations with a lipid bilayer mimicking the composition of the inner leaflet of the *A. baumannii* outer membrane (12% cardiolipin, 16% phosphatidylglycerol [PG], and 72% phosphatidylethanolamine [PE] [see Materials and Methods]). The enzymes were triacylated at their N-terminal cysteine residue, as suggested by the bioinformatic analysis of the signal peptide. In all simulations (five MD replicas) both enzymes readily anchored into and kept attached to the lipid bilayer via the triacyl moiety in their N-terminus. OXA-23 and OXA-24/40 adopted similar orientations on the membrane, laying their globular domain on its surface while leaving their active site facing the periplasmic space (Movies S1 and S2; Fig. 2).

This positioning of OXA-23 and OXA-24/40 might be a structural feature that prevents the occlusion of their active site by interaction with the lipid bilayer, as the same phenomenon has been observed in MD studies of lipidated NDM-1 (36).

Cardiolipin molecules displayed considerably high contact frequency (percentage of the simulation time) with the globular domain of OXA-24/40, despite representing only 12% of the membrane's lipid composition, notably with residues Arg151 (56.9%), Arg190 (53.8%), Lys61 (53.2%), Lys150 (45%), and Lys147 (43.3%) (Fig. 2B). Albeit to a lesser extent, the residues in the analogous positions in OXA-23 also helped stabilize the enzyme's conformation on the membrane surface via cardiolipin interactions as measured by contact frequency: Arg149 (26.9%), Lys148 (25%), Lys145 (21.9%), and Lys60 (20.1%) (Fig. 2B). Despite not being essential for membrane anchoring, these electrostatic interactions could help orient OXA-23 and OXA-24/40 in such a way that their active sites remain available for substrate binding.

OXA-23 and OXA-24/40 are lipidated, membrane-anchored proteins

To experimentally test the bioinformatic predictions and the molecular simulations, we performed cellular fractionation experiments. We selected the two putative lipidated OXA-23 and OXA-24/40 expressed in *A. baumannii*, and a putative soluble periplasmic OXA, OXA-48, lacking a lipobox sequence and commonly produced by Enterobacterales

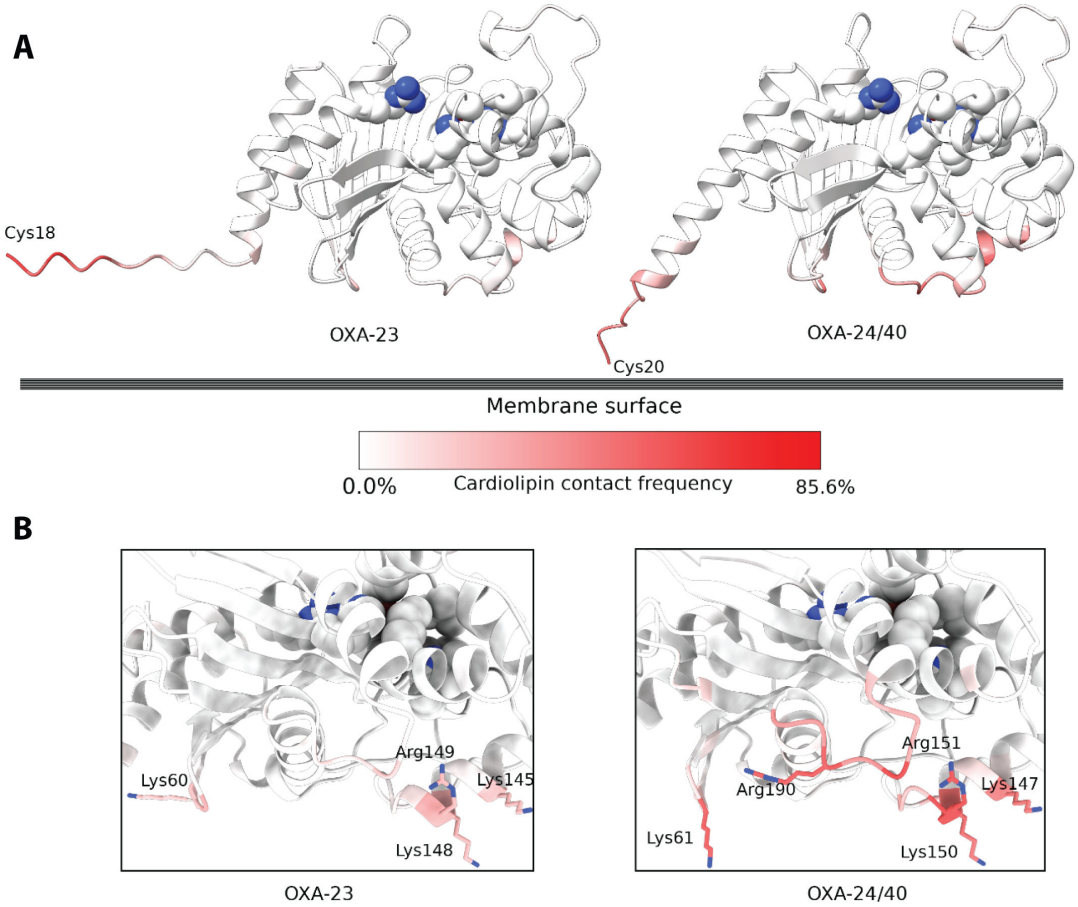

FIG 2 Residue-wise contact frequency (%) with cardiolipin lipids during the simulations. (A) OXA-23 and OXA-24/40 contact frequency (measured as percentage of simulation time) with cardiolipin, color-coded from white (0% frequency) to red (85.5% frequency). The lipidated cysteines (Cys18 and Cys20) are indicated in the N-terminus of both β-lactamases. Active site residues are shown as spheres. (B) A close-up of the residues (shown as sticks) on the opposite side of the active site (shown as spheres). These positively charged residues also contribute to membrane binding, positioning the active site toward the periplasm and preventing its occlusion.

such as *K. pneumoniae* and *E. coli* (Fig. 3A) (12). All these selected proteins are clinically relevant carbapenemases (1, 9).

These three proteins were expressed by the pMBLe_OA plasmid with their native signal peptides and with a Strep-tag (ST) fused to the C-terminal to allow uniform immunodetection (37). We chose *A. baumannii* ATCC 17978 and *E. coli* ATCC 25922 as laboratory strains for the different organisms with isogenic backgrounds. The grown cells were subjected to a cell fractionation assay, which allowed collecting the periplasmic fraction (Per) after treatment with lysozyme. Sonication then led to the separation of total membranes (40) from the cytoplasm (Cyt). Whole cells (WC) and each fraction were analyzed by immunoblotting with anti-ST antibodies for the β-lactamases. Specific antibodies against cytoplasmic RNA polymerase (RNApol) and the outer membrane protein A (OmpA), were used as controls for the quality of the preparation of the soluble and membrane fractions, respectively. Figure 3B shows that OXA-23 and OXA-24/40 were present in the membrane fractions of *A. baumannii*, with no accumulation of these proteins in the periplasmic fraction. In contrast, OXA-48 was detected only in the periplasmic fraction of *E. coli* as a soluble β-lactamase (Fig. 3B).

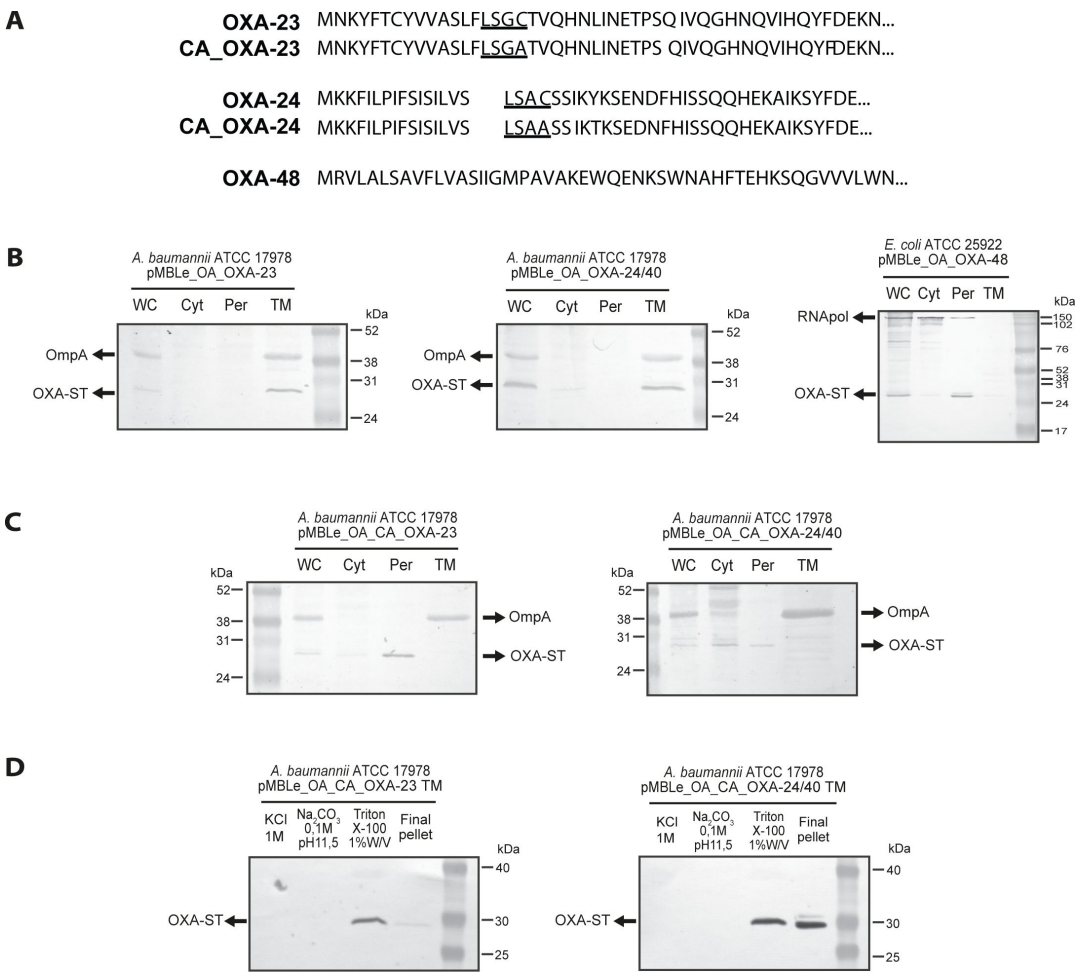

FIG 3 OXA-23 and OXA-24/40 are membrane-anchored proteins, while OXA-48 is soluble periplasmic. (A) N-terminal sequences of the OXAs object of the experimental analysis. The lipoboxes are underlined and the cysteine target of lipidation is bolded. (B) Cell fractionation of *A. baumannii* ATCC 17978 expressing OXA-23 and OXA-24/40, and *E. coli* ATCC 25922 expressing OXA-48. (C) Cell fractionation of *A. baumannii* expressing the Cys18Ala-OXA-23 (CA_OXA-23) and Cys20Ala-OXA-24/40 (CA_OXA-24/40) variants. (D) Solubilization assays of OXA-23 and OXA-24/40 from *A. baumannii* total membranes. OXA-ST indicates the bands corresponding to anti-ST antibodies, which match the molecular weight of the enzymes fused to the tag. OmpA indicated the bands revealed by anti-OmpA antibodies which recognize the outer membrane protein OmpA. RNApol indicated the bands revealed using RNA polymerase antibodies.

The lipobox is a signature sequence of bacterial lipoproteins, and the cysteine residue located at its C-terminus is the target of lipidation. To confirm the role of this residue in the localization in the membrane fraction of OXA 23 and OXA-24/40 in *A. baumannii*, we substituted the Cys for Ala in both proteins (Cys18 in OXA-23 and Cys20 in OXA-24/40) (Fig. 3A) and analyzed the impact of this replacement in the cellular localization of both enzymes. Expression of the Cys18Ala_OXA-23 (CA_OXA-23) and Cys20Ala_OXA-24/40 (CA_OXA-24/40) variants in *A. baumannii* resulted in the accumulation of both proteins only in the periplasmic fractions as soluble proteins, separately from OmpA, which is present in total membrane fractions, confirming our hypothesis (Fig. 3C).

To assess the nature of the interaction between the bacterial membrane and OXA-23 and OXA-24/40, we attempted to solubilize these enzymes from the pure *A. baumannii* membranes using different methods. Treatment with high ionic strength (1 M NaCl) and highly basic pH (0.1 M Na_2CO_3 pH 11.5) did not release any of the two OXAs from the membrane fractions (Fig. 3D), indicating that they are not peripheral proteins associated with the membrane by only means of electrostatic interactions, although these interactions can better expose the active side to the periplasmic space, as observed with MD simulations (Fig. 2). Instead, OXA-23 and OXA-24/40 were only solubilized upon treatment with 1% wt/vol Triton X-100 (Fig. 3D), confirming that both enzymes interact with the membrane through hydrophobic interactions. Overall, these results establish that OXA-23 and OXA-24/40 are lipidated, membrane-bound proteins in *A. baumannii*.

The MIC values of piperacillin and imipenem against *A. baumannii* cells expressing the soluble and membrane-bound variants of both OXA-23 and OXA-24/40 were similar (Table S3), revealing that the cell localization does not contribute to the resistance phenotype.

Lipidated OXAs are selectively secreted into OMVs

We then explored whether membrane anchoring of OXAs results in packaging into OMVs. We purified OMVs from *A. baumannii* expressing native OXA-23 and OXA-24/40, and the soluble variants CA_OXA-23 and CA_OXA-24/40 and quantified the protein levels in the vesicles. Despite the protein levels of lipidated and soluble variants were comparable in WCs, only the lipidated OXAs were incorporated at high levels in OMVs from *A. baumannii* (Fig. 4A). Figure 4B shows that removal of the lipidation site for CA_OXA-23 leads to a substantial decrease of approximately 95% in the transported enzyme by vesicles. Similarly, in the case of CA_OXA-24/40, there is an approximately 85% reduction in the level of the enzyme into OMVs, indicating that membrane anchoring contributes to the selective secretion of OXA-23 and OXA-24/40 in *A. baumannii* cells.

To assess whether the OXA enzymes are located in the lumen of the vesicles or pointing outwards, we exposed the OXA-loaded vesicles to proteinase K to assess the accessibility of this protease to the enzymes in the OMVs. Treatment of the intact vesicles with proteinase K did not alter the levels of OXA-23 or OXA-24/40. Instead, both enzymes were completely degraded by proteinase K in Triton-lysed vesicles (Fig. 4C). These experiments suggest that the proteins are located in the lumen of the OMVs, confirming the protective role of the vesicles from extracellular degradation when these enzymes are secreted.

OXA-loaded OMVs protect β-lactam-susceptible bacteria

We then attempted to determine if the OXAs incorporated into vesicles were in their active forms by examining the protective effect of β-lactamase-loaded vesicles in β-lactam-susceptible bacteria. We tested this in β-lactam-susceptible *A. baumannii*, *E. coli*, and *Pseudomonas aeruginosa* cells treated with OMVs from *A. baumannii* carrying the empty vector (EV) or expressing OXAs in the presence of imipenem or piperacillin, and we determined the MICs.

Incubation of β-lactam-susceptible *A. baumannii* with OMVs loaded with lipidated OXA-24/40 resulted in a MIC against imipenem of 32 µg/mL versus a MIC of 2 µg/mL for

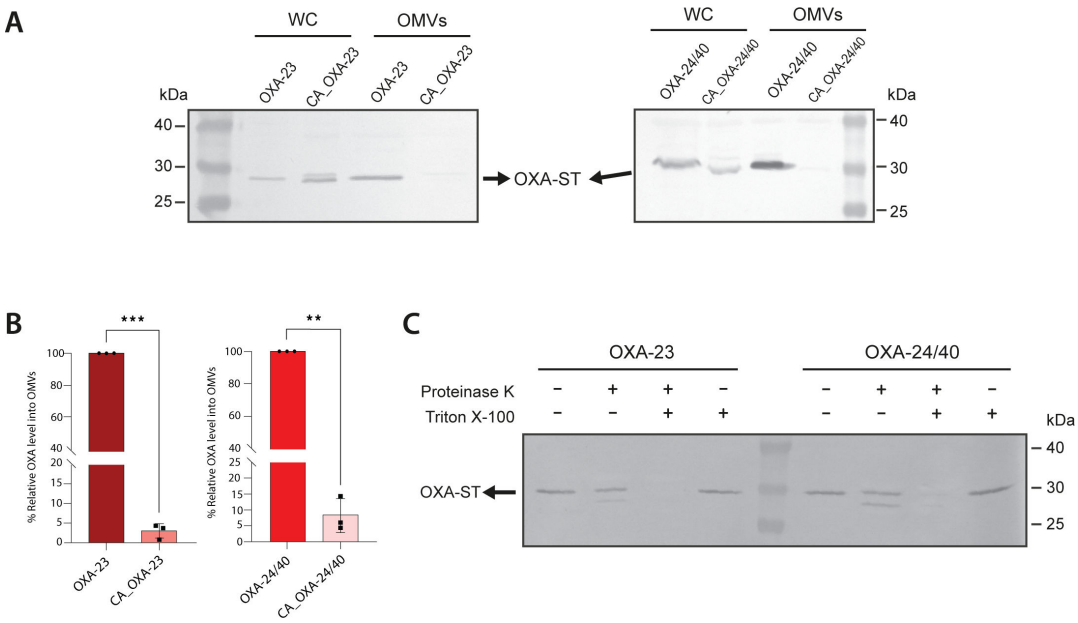

FIG 4 Membrane-anchored OXAs are incorporated in higher proportions into OMVs than periplasmic soluble OXAs. (A) Anti-ST immunoblotting of whole cells (WCs) and outer membrane vesicles (OMVs) from *A. baumannii* ATCC 17978 expressing OXA-23 or OXA-24/40 and its soluble variants (CA_OXA-23 or CA_OXA-24/40). (B) Comparison between the percentages (%) of the levels of the soluble variants CA_OXA-23 and CA_OXA-24/40 into OMVs. The plotted values, normalized to the corresponding wild-type OXA (lipidated OXA) levels, were obtained as described in Materials and Methods. Data correspond to three independent experiments (black-filled symbols) and are shown as the mean value. Error bars represent standard deviations (SDs). *P* values according to the Student's *t* test: $^{**}P \leq 0.01$, $^{***}P \leq 0.001$. (C) Anti-ST immunoblotting of OMVs from *A. baumannii* carrying OXA-23 or OXA-24/40 treated with and without Proteinase K and 1% vol/vol Triton X-100.

those cells incubated with vesicles loaded with the soluble variant, and a MIC of 0.125 µg/mL for control vesicles isolated from *A. baumannii* cells transformed with the empty plasmid (Fig. 5A; Table S4). The same trend was observed for β-lactam-susceptible *E. coli* and *P. aeruginosa* cells and for OXA-23 and its soluble variant. In this case, the β-lactam-susceptible *A. baumannii* cells grew at 8 µg/mL imipenem when incubated with OXA-23-containing OMVs versus 1 µg/mL imipenem for vesicles loaded with the soluble variant CA_OXA-23 (Fig. 5A; Table S4). A similar protection effect was observed for piperacillin, with a high impact in the MICs for the three tested β-lactam-susceptible bacteria when were incubated with OMVs loaded with lipidated OXAs (Fig. 5B; Table S4). The trend of enhanced protection with a higher MIC when using OXA-24/40-loaded vesicles compared to OXA-23-loaded vesicles is likely attributed to the higher levels of OXA-24/40 in the concentration of OMVs used during the incubation experiment with susceptible bacteria. In fact, the levels of OXA-24/40 in the OMVs were approximately four times higher than those of OXA-23. Overall, these results indicate that OXA enzymes are active within vesicles produced by *A. baumannii*, playing a collective role in improving the viability of antibiotic-susceptible bacteria and that this role is highly dependent on the membrane localization of these enzymes.

DISCUSSION

Antimicrobial resistance (AMR) is an inevitable consequence of the use of antibiotics. β-lactamases represent the predominant mechanism of resistance to β-lactam antibiotics, as accounted by the early report of a penicillinase in 1940 before the clinical use of antibiotics (41). In the current century, we have witnessed an alarming spread of resistance genes coding for β-lactamases among pathogenic and opportunistic bacteria, with >8,000 variants reported so far. Biochemistry and structural studies have described the mechanistic and structural features eliciting resistance to new drugs (42). However, there are still many aspects incompletely understood about the biochemical

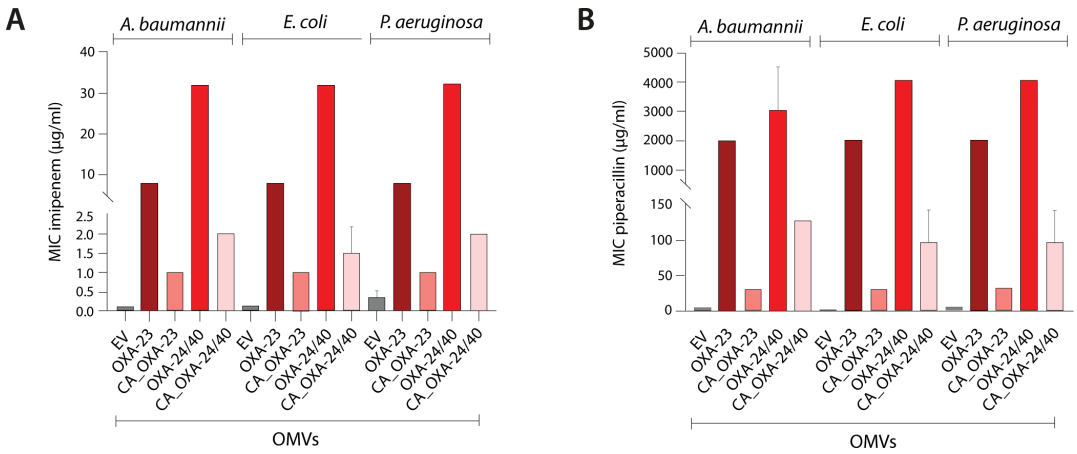

FIG 5 OMVs loaded with lipidated OXAs provide enhanced protection to β-lactam-susceptible bacteria than OMVs containing soluble variants. MIC values (µg/mL) against (A) imipenem and (B) piperacillin of β-lactam susceptible *A. baumannii*, *E. coli*, and *P. aeruginosa* cells after treatment with OMVs purified from *A. baumannii* carrying empty vector (EV) or expressing lipidated enzymes: OXA-23 or OXA-24/40 or soluble enzymes: CA_OXA-23 or CA_OXA-24/40. Data correspond to mean values from two independent experiments. Error bars represent standard deviations (SD). The MICs of susceptible bacteria against imipenem or piperacillin (without incubation with OMVs) are shown in Table S3.

and mechanistic aspects of β-lactamases. Indeed, the catalytic mechanism of MBLs was dissected only 5 years ago (43), and a recent paper disclosed the role of anions in the biphasic nature of the kinetics of OXA enzymes (44, 45).

In addition to these biochemical issues, host-specific aspects of β-lactamases are poorly understood. For example, it is not clear why some enzymes, despite being plasmid-borne, are confined to some bacterial host(s), while others are present in a wider variety of microorganisms. This phenomenon has been recently addressed in the case of MBLs (46), but it is not defined for serine-dependent enzymes. Finally, the bacterial physiology of β-lactamases in the periplasm of Gram-negative bacteria is scarcely characterized, a problem that includes the incomplete knowledge of the cellular localization of these enzymes, which can be soluble or membrane-bound. The latter was shown to be the case of NDM-1 and its different allelic variants (47). The cellular localization of NDM variants improves the stability of these enzymes and favors their incorporation into OMVs from different bacteria (19, 46).

The identification of a lipobox sequence helps annotate a protein as putative lipidated and membrane-bound. In this work, we examined the distribution of lipoboxes in the signal peptides of β-lactamases from all four classes. We found that the distribution of putative lipidated enzymes is diverse, depending on the class of β-lactamase and the microorganism. Within the Class A group, representing one-fourth of reported β-lactamases, only 15% of enzymes contain lipoboxes. Two of them, BRO from *M. catarrhalis* and PenI from *B. pseudomallei*, have already been characterized biochemically. Within Class B, all NDM variants are membrane-bound (68 out of >800 enzymes), which have been reported in Enterobacterales and non-fermenters. Instead, Class D enzymes are singular since 60% of the OXA β-lactamases contain a lipobox, all of them (with only one exception) being expressed in *Acinetobacter* spp. This suggests a host-specific effect for these enzymes that contrasts with the host distribution of lipidated Class A and Class B β-lactamases.

Coarse-grained MD simulations predict that the lipid moiety attached to a Cys residue in the lipobox of OXA-23 and OXA-24/40 is inserted in the lipid bilayer in such a way that a patch in the globular domains of these enzymes presents an attractive interaction with the bacterial membrane. This interaction is expected to favor and stabilize membrane binding as well as to orient the enzyme active site toward the periplasm.

We validated these predictions by cellular fractionation and immunoblotting experiments, that reveal that OXA-23 and OXA-24/40 are lipidated, membrane-bound

proteins in *Acinetobacter* spp. Mutagenesis of the Cys residue in the lipobox gives rise to soluble proteins in both cases. We also studied as a control OXA-48 (lacking a lipobox), a soluble, periplasmic enzyme in *E. coli*.

Both OXA-23 and OXA-24/40 were secreted into OMVs from *A. baumannii*. In both cases, the soluble variants resulting from a mutation at the lipobox were also secreted into OMVs, but to a much smaller content. This behavior is similar to what has been reported for NDM, that is, membrane anchoring significantly facilitates secretion into vesicles, but the soluble variants can also be secreted (19). Incubation of different antibiotic-susceptible bacteria with OXA-loaded OMVs resulted in a protective effect of these bacteria against carbapenem and penicillin. In all cases, the protective effect (measured as an increase in the MIC) correlates with the amount of protein present in the OMVs. This reveals that both OXA-23 and OXA-24/40 are secreted in their active form, as is the case for NDM-1.

The current results help unify many findings in the literature and coalesce different observations. OXA-23 has been shown to display an extensive interaction network in *A. baumannii* by cross-linking and mass spectrometry experiments (48). OXA-23 interacts with the outer membrane proteins OmpA, OmpW, CarO, and ABUW_2898, as well as with YiaD, an outer membrane protein that has been related to carbapenem resistance. In all these cases, the cross-linking was observed through residue Lys60 in OXA-23, which is one of the positively charged residues in the protein surface identified as making transient interactions with the outer membrane (Fig. 2). We propose that the reported interaction (48) is due to the proximity of OXA-23 to the outer membrane.

A proteomics analysis of OMVs from the multidrug-resistant clinical isolate *A. baumannii* DU202 revealed that OXA-23 accounted for 36% of the total protein content in OMVs (49). Thus, despite the relatively low levels of expression of OXA-23 in the current model organism, secretion of OXA β-lactamases into OMVs in clinical strains can be a relevant phenomenon. Liao et al. (50) informed the finding of OXA-58 in the lumen of OMVs from *A. baumannii* Ab290. Our analysis (Table 2) predicts the OXA-58 family as lipidated, also supporting this finding.

OMVs have been suggested to play different roles in bacteria. These vesicles are essential in cellular detoxification processes, by removing toxic periplasmic components that elicit envelope stress and compromise bacterial fitness. This has been shown to be the case for some Class B β-lactamases when expressed in non-frequent bacterial hosts, such as VIM-2 and SPM-1 (46). Colquhoun et al. recently observed that hyperexpression of OXA-23 in *A. baumannii* induces collateral physiological damages by altering the peptidoglycan integrity (51). We postulate that the incorporation of OXA-23 into OMVs might mitigate the negative impact of OXA-23 overexpression by reducing the effective concentration of OXA-23 in the periplasm, at the same time increasing the levels of this β-lactamase in the environment by its presence in OMVs, thus contributing to resistance.

We also show here that OXA-loaded vesicles are able to protect bacterial populations of otherwise susceptible *A. baumannii*, *P. aeruginosa*, and *E. coli* from the activity of β-lactam antibiotics. Therefore, the expression of lipidated OXA enzymes may provide an advantage both for the producing organism and in polymicrobial infections. Indeed, multidrug-resistant *Acinetobacter* spp. is increasingly reported in co-colonization events in intensive care units with Enterobacterales expressing extended-spectrum β-lactamases (ESBLs) (52–54). A recent analysis from Semenec et al. (55) has described the relevance of cross-protection of *A. baumannii* on *K. pneumoniae* against cefotaxime in a polymicrobial lung infection. In addition, this protein-mediated protection effect could be coupled to plasmid transfer. The seminal work from Bou et al. reported the role of OMVs in transferring the plasmid containing the $bla_{\text{OXA-24/40}}$ gene between different *A. baumannii* strains (56). Overall, this calls for a deeper understanding of the role of OMVs in polymicrobial infections through studies able to assess the biochemical bases of cross-protection, including the presence of different β-lactamases as selective vesicle cargo.

In closing, this work also underscores the relevance of studying the physiology of β-lactamases in their native bacterial hosts when using model organisms with isogenic backgrounds. The identification of a large, clinically relevant family of β-lactamases as membrane-bound proteins in *A. baumannii* linked to their presence in vesicles requires us to address novel approaches to clinical treatments, particularly in polymicrobial infections.

MATERIALS AND METHODS

Bioinformatic analysis

The Entrez module from the Biopython library (57) was used to access the FASTA sequences from the NCBI database using the accession codes listed in the "GenPeptID" column of the β-lactamase database (3). The ignore list command was utilized to exclude entries containing dashes, blank spaces, "assigned," and "Withdrawn." For enzymes with multiple accession numbers, the first one listed was selected. All sequences were compiled into a list, which was then saved as a text file. The Python script is available upon request. The generated file was used as the input for the SignalP 6.0 server available at https://services.healthtech.dtu.dk/services/SignalP-6.0. The prediction was executed in slow mode, with "short output" and "Other" selected as the organism option. The results were downloaded as a JSON summary, copied into Table S1, and aligned with the information from the β-lactamase database.

CG-MD simulations

Structures of OXA-23 and OXA-24/40 were obtained from the AlphaFold Protein Structure Database (AFDB) (58) under the UniProt accession codes A0A068J749 and Q8RLA6, respectively (59). This was done as the structures of these enzymes deposited in the Protein Data Bank (PDB) (60) lacked a considerable portion of both proteins' N-terminal sequence, including the cysteine residue that is lipidated. Nonetheless, the globular domains of both enzymes' models were inspected and compared to their deposited structures, confirming that the models had excellent accuracy (OXA-23 AF model pLDDT = 95.7, RMSD against PDB ID 4JF4 = 0.427 Å; OXA-24/40 AF model pLDDT = 95.7, RMSD with PDB ID 3ZNT = 0.208 Å). The models in the AFDB are computed based on the proteins' complete sequence, so it was necessary to remove the signal peptides of both OXA-23 (up to Cys18) and OXA-24/40 (up to Cys20).

The simulations were performed using the MARTINI 3.0 forcefield (40). The first step involved the coarse-graining of the protein models done using the Martinize 2 tool (61). An elastic network with a bond force constant of 500 kJ mol^{-1} nm^{-2} and lower and upper elastic bond cutoffs of 0.5 and 0.9 nm, respectively, were implemented to stabilize the tertiary structure of the proteins. The parameters and structure of the triacyl moiety covalently attached to the N-terminus cysteine were taken from Rao et al. (62), who also made available a Python script to generate an initial configuration for the lipidated residue. The INSert membrANE (*insane*) program (63) was used to build the simulation systems: a tetragonal box of dimensions $13 \times 13 \times 15$ nm^3 (X, Y, Z) containing a symmetric lipid bilayer of 72% POPE, 16% POPG, and 12% cardiolipin, mimicking the composition of the *A. baumannii* OM inner leaflet (64). The systems were immersed in water with either OXA-23 or OXA-24/40 positioned 7 nm away from the membrane surface. The parameters for cardiolipin were obtained from Corey et al. (65), while the other lipids were already included in the official release of the MARTINI 3.0 force field. The systems were then neutralized with Na^+ counter ions.

GROMACS (66) version 2022.1 was used to run all the MD simulations. In all stages of the procedure, the cutoff radius for short-range electrostatic and van der Waals interactions was 11 Å. The reaction field method (67) was implemented to calculate long-range electrostatic interactions. Periodic boundary conditions were applied in all directions. Energy minimization and equilibration of the systems was performed as per

the recommended protocol of the CHARMM-GUI web server (68) as of July 2023. The production dynamics were performed in the NPT ensemble, with the V-rescale thermostat (69) and the Parrinello-Rahman barostat (70). Both systems had five replicas and each ran for 4 µs. Protein-lipid interaction analyses were performed with the ProLint Web Server (71), using an interaction cutoff of 6 Å. The visual molecular dynamics (VMD) (72) software was used for visual inspection of the simulations and recording of the movies. All protein and membrane images were generated with ChimeraX (73).

Bacterial strains, culture conditions, and plasmid constructions

E. coli ATCC 25922 and *A. baumannii* ATCC 17978 were used for expression of the EV pMBLe-OA and also for expression of the different OXAs. The bla_{OXA} genes were cloned into the pMBLe-OA vector (46) fused to a Strep-Tag II sequence and downstream of a pTac promoter inducible by isopropyl β-D-1-thiogalactopyranoside (IPTG). All strains were grown aerobically at 37°C in lysogeny broth (LB) medium supplemented with gentamicin 20 µg/mL when necessary. Expression of the enzymes was induced at OD = 0.4 by adding 10 µM IPTG and incubated for 4 h at 37°C.

Chemical reagents were purchased from Sigma-Aldrich.

Variant constructions by PCR overlap

The soluble variants of OXA-23 and OXA-24/40 were constructed by site-directed mutagenesis using overlapping primers. For each enzyme, we amplified the full-length bla_{OXA} genes, including their native signal peptides from a pUC57 (Macrogen) plasmid using mutagenic primers and internal plasmid primers called pMBLe_Fw 5′-GCTGTTGACAATTAATCATCGGCTC-3′ and pMBLe_Rv 5′-CGTAGCGCCGATGGTAGTG-3′.

To construct CA_OXA-23 we used the following couple of primers: pMBLe_Fw 5′-AAATTATGCTGAACCGTAGCACCAGAAAGAAAAAG-3′ and pMBLe_Rv 5′-CTTTTTCTTTCTGGTGCTACGGTTCAGCATAATTT-3′. The double-stranded DNA obtained and the plasmid pMBLe were cleaved using *Nde*I and *Eco*RI and therefore ligated. Then, pMBLe-OXA-23 was digested with *Bam*HI and *Eco*RI and ligated with pMBLe_OA digested with the same enzymes.

To construct CA_OXA-24/40, we used the following series of primers: pMBLe_Fw 5′-AGTTTTAATAGATGAAGCTGCACTGAGAGAAACTAG-3′ and pMBLe_Rv 5′-CTAGTTTCTCTCAGTGCAGCTTCATCTATTAAAACT-3′. The double stranded DNA obtained and the plasmid pMBLe were cleaved using *Nde*I and *Hind*III and were then ligated. Molecular biology enzymes were purchased from Thermo-Fisher, and primers were ordered from Invitrogen.

Cell fractionation

The fractionation protocol was based in the one described by Pettiti et al. (74). The cells were pelleted and resuspended in 0.2 M Tris at pH 8, 1 M sucrose, 1 mM EDTA in a proportion of 10 mL per initial culture liter. Lysozyme 1 mg/mL was added and incubated for 5 mins at room temperature. The suspension was centrifuged at 30,000 × *g* for 20 min, resulting in a supernatant containing the periplasmic fraction and a pellet containing the spheroplast and membrane remains. The pellet was resuspended in 10 mM Tris at pH 8.5 EDTA 2.5 mM 10 µg/mL DNAse 1 mM PMSF and sonicated. Once cell debris was removed, the suspension was ultracentrifuged at 45,000 × *g* for 45 min. The supernatant containing the cytoplasm was collected. The pelleted total membrane was resuspended in 10 mM Hepes, 0.2 M NaCl at pH 7.5. The resuspension volumes were normalized according to the OD_{600} and the initial culture volume.

Selective membrane protein solubilization

Membrane proteins were extracted sequentially. First, the total membrane fraction was pelleted by ultracentrifugation at 45,000 × *g* for 45 min and gently resuspended in

cold 1 M KCl. After 30 min incubation on ice, they were ultracentrifuged again. The supernatants containing loosely associated peripheral proteins were collected and the pellets were resuspended in 0.1 M Na_2HCO_3 at pH 11.5. After a 30-min incubation on iceto release peripheral proteins associated with strong electrostatic interactions were centrifugated again. The pellets were resuspended in 1% wt/vol Triton X-100 and incubated for 30 min on ice to extract integral or hydrophobically associated proteins in detergent micelles. The supernatants were collected, and the pellets were resuspended in 10 mM Hepes, 0.2 M NaCl at pH 7.5.

Protein immunodetection

Immunoblotting assays were realized in polyvinylidene difluoride (PVDF) membranes using Strep-Tag II monoclonal antibodies (at 1:1,000 dilution from a 200 µg/mL solution) (Novagen) and immunoglobulin G-alkaline phosphatase conjugates (at 1:5,000 dilution). Monoclonal anti-RNApol was used as a cytoplasmic control and polyclonal anti-OmpA kindly provided by Dr. Alejandro Viale was used as a membrane marker.

The WCs, periplasm, and cytoplasm samples were normalized according to the following equation: V = 100 µL× OD_{600} × V_c, where V_c is the starting volume of culture sample. Total membrane fraction and OMVs were normalized according to a lipid quantification by FM4-64 (Thermofisher). Protein band intensities were quantified by using Gel Analyzer software (75).

Purification of OMVs and OXA level detection in OMVs

Overnight cultures of *A. baumannii* pMBLe-OA-*bla* cells were grown in 300 mL of LB broth at 37°C, reaching an OD_{600} of 0.4. Subsequent induction with 20 µM IPTG was followed by continued overnight growth with agitation. The cells were harvested, and the supernatant was filtered through a 0.45 µM membrane (Millipore). Ammonium sulfate was added to the filtrate at a concentration of 55% (wt/vol), followed by overnight incubation with stirring at 4°C. Precipitated material was separated by centrifugation at 12,800 × *g* for 10 min, resuspended in 10 mM HEPES, 200 mM NaCl at pH 7.4, and dialyzed overnight against >100 volumes of the same buffer. Next, samples were filtered through a 0.45 µM membrane, layered over an equal volume of 35% (wt/vol) sucrose solution, and ultracentrifuged at 150,000 × *g* for 1 h and 4°C. Pellets containing the OMVs were washed once with 10 mM HEPES, 200 mM NaCl at pH 7.4, and stored at −80°C until use.

The OMVs were quantified by two different methods. The total protein concentration was measured by the Pierce bicinchoninic acid (BCA) protein assay kit (Thermo Scientific) as described (37). Lipid content associated with OMVs was determined using the lipophilic fluorescent dye FM4-64 (Thermofisher) as described previously (76). Briefly, a portion of OMVs was incubated with FM4-64 (2 µg/mL in PBS) for 10 min at room temperature. Separate samples of OMVs and the FM4-64 probe were used as negative controls. After excitation at 515 nm, emission at 640 nm was measured with the multiplate reader SYNERGY HT (Biotek).

The OMV content was analyzed by SDS-PAGE and immunoblotting. Gel lanes were equally loaded based on total protein and lipid content. The pre-stained *Blue Plus II* Protein Marker (14–120 kDa) provided molecular weight standards for Fig. 4. To determine the levels of OXA-23, CA_OXA-23, OXA-24/40, and CA_OXA-24/40 in OMVs, the mature protein band intensities in WCs and in the OMVs, derived from *A. baumannii* expressing each OXA protein, were quantified from PVDF membranes using GelAnalyzer software (53). The quantity of each OXA protein in the OMVs (from immunoblots) was divided by the quantity of each OXA in WCs (from immunoblots). Finally, the values plotted in Fig. 4B (expressed as a percentage) correspond to the normalization of the levels of each soluble OXA (CA_OXA-23 or CA_OXA-24/40) to the value of its corresponding wild-type OXA (OXA-23 or OXA-24/40), which was taken as 100%.

Proteinase K accessibility assay

OMVs were resuspended in a buffer containing 10 mM Tris HCl (pH 8) and 5 mM $CaCl_2$. When required, OMVs were lysed by incubation with 1% (vol/vol) Triton X-100 for 30 min at 37°C. Intact and lysed OMVs were incubated for 60 min at 37°C in the presence of 100 µg/mL proteinase K. The reaction was stopped by the addition of 5 mM phenylmethanesulfonyl fluoride (PMSF), and samples were analyzed by SDS-PAGE and immunoblotting.

MICs of OXA-23, CA_OXA-23, OXA-24, and CA_OXA-24

To determine MICs (µg/mL) of the β-lactam antibiotics imipenem and piperacillin (Sigma-Aldrich) on strains of *A. baumannii* carrying OXAs, we followed the standard agar plate protocol recommended by the CLSI.

Effect of OMVs loaded with OXAs on MICs of bacteria

To determine the MICs (µg/mL) of the β-lactam antibiotics imipenem and piperacillin (Sigma-Aldrich) on β-lactam-susceptible strains of *A. baumannii*, *E. coli*, and *P. aeruginosa* after treatment with OMVs, we utilized OMVs purified from *A. baumannii* carrying an EV or expressing either lipidated (OXA-23 or OXA-24/40) or soluble enzymes (CA_OXA-23 or CA_OXA-24/40). We determined the MIC by broth‐dilution method in 96‐well plates according to the CLSI guidelines. β-lactam-susceptible cells (5×10^5 CFU/mL) were inoculated into medium without β-lactam or with twofold increasing concentrations of imipenem or piperacillin, and with 1 µg/mL of OMVs from *A. baumannii* carrying an EV or expressing OXAs. The 96-well plates were incubated at 37°C with constant shaking and the OD was recorded at 600 nm at 30 min time intervals, using a Biotek Epoch 2 microplate reader. MIC values were measured from two independent experiments.

ACKNOWLEDGMENTS

This research was supported by grants from the National Institutes of Health (R01AI100560 to R.A.B. and A.J.V.), Agencia I+D+I (PICT-2020-00031 to A.J.V.), MinCyT (REPARA to A.J.V.), the European Union's Horizon 2020 research and innovation program under the Marie Skłodowska-Curie (grant agreement no. 945363 to F.T.P.M.), and the Swiss National Science Foundation (CRSII5_198737 to M.D.P.). A.J.V. and C.L. are staff members from CONICET. L.C. is the recipient of a fellowship from CONICET, Argentina. F.T.P.M. and M.D.P. are staff members of EPFL.

We thank Marina Avecilla (IBR-CONICET) for her excellent technical assistance.

C.L. and A.J.V. designed the research and supervised the study. L.C. and G.B. performed the bioinformatics analysis of the lipobox sequences. L.C. performed plasmid constructions for OXAs and their soluble variants, cell fractionation and protein localization, selective membrane solubilization, and OXA immunodetection. C.L. performed OMVs purification, detection, and determination of OXA levels into OMVs, proteinase K assay, and protection assay with OMVs. F.T.P.M. performed the molecular simulation experiments. L.C., C.L., and F.T.P.M. designed the figures. All authors analyzed data, discussed results, and contributed and edited manuscript.

The content is solely the responsibility of the authors and does not necessarily represent the official views of the National Institutes of Health or the Department of Veterans Affairs.

AUTHOR AFFILIATIONS

[1]Instituto de Biología Molecular y Celular de Rosario (CONICET IBR -UNR), Rosario, Argentina
[2]Área Biofísica, Facultad de Ciencias Bioquímicas y Farmacéuticas, Universidad Nacional de Rosario, Rosario, Santa Fe, Argentina

[3]Institute of Bioengineering, School of Life Science, École Polytechnique Fédérale de Lausanne (EPFL), Lausanne, Switzerland
[4]Department of Molecular Biology and Microbiology, Case Western Reserve University School of Medicine, Cleveland, Ohio, USA
[5]Research Service, Louis Stokes Cleveland Department of Veterans Affairs Medical Center, Cleveland, Ohio, USA
[6]Departments of Pharmacology, Biochemistry, Proteomics and Bioinformatics, Case Western Reserve University School of Medicine, Cleveland, Ohio, USA
[7]CWRU-Cleveland VAMC Center for Antimicrobial Resistance and Epidemiology (Case VA CARES), Cleveland, Ohio, USA

PRESENT ADDRESS

Guillermo Bahr, Terragene, Parque Industrial Micropi, Alvear, Argentina

AUTHOR ORCIDs

Lucia Capodimonte http://orcid.org/0009-0005-5585-9239
Robert A. Bonomo http://orcid.org/0000-0002-3299-894X
Carolina López http://orcid.org/0000-0002-9357-3486
Alejandro J. Vila http://orcid.org/0000-0002-7978-3233

FUNDING

Funder	Grant(s)	Author(s)
HHS | NIH | National Institute of Allergy and Infectious Diseases (NIAID)	R01AI100560	Robert A. Bonomo Alejandro J. Vila
Agencia Nacional de Promoción de la Investigación, el Desarrollo Tecnológico y la Innovación (Agencia I+D+i)	PICT-2020-00031	Alejandro J. Vila
Ministerio de Ciencia, Tecnología e Innovación (MINCyT)	REPARA (Red Federal 115)	Alejandro J. Vila
EC | Horizon Europe | Excellent Science | HORIZON EUROPE Marie Sklodowska-Curie Actions (MSCA)	945363	Fernando Teixeira Pinto Meireles
Swiss National Science Foundation	CRSII5_198737	Matteo Dal Peraro

AUTHOR CONTRIBUTIONS

Lucia Capodimonte, Conceptualization, Investigation, Methodology, Validation, Visualization, Writing – original draft, Writing – review and editing | Fernando Teixeira Pinto Meireles, Investigation, Methodology, Visualization, Writing – original draft, Writing – review and editing | Guillermo Bahr, Conceptualization, Investigation | Robert A. Bonomo, Funding acquisition, Writing – original draft, Writing – review and editing | Matteo Dal Peraro, Conceptualization, Funding acquisition, Methodology, Supervision, Writing – original draft, Writing – review and editing | Carolina López, Conceptualization, Data curation, Formal analysis, Investigation, Methodology, Supervision, Writing – original draft, Writing – review and editing | Alejandro J. Vila, Conceptualization, Formal analysis, Funding acquisition, Project administration, Supervision, Writing – original draft, Writing – review and editing

DIRECT CONTRIBUTION

This article is a direct contribution from Alejandro J. Vila, a Fellow of the American Academy of Microbiology, who arranged for and secured reviews by Cesar A. Arias,

Houston Methodist Hospital and Weill Cornell Medical College, and Sergei B. Vakulenko, University of Notre Dame.

ADDITIONAL FILES

The following material is available online.

Supplemental Material

Supplemental Legends (mBio03343-24-s0001.docx). Legends for Tables S1 to S2 and Movies S1 and S2.
Table S1 (mBio03343-24-s0002.xlsx). Bioinformatics analysis of the cellular localization of β-lactamases from all four classes based on the signal peptide.
Table S2 (mBio03343-24-s0003.docx). Predicted cellular localization of class D β-lactamases.
Table S3 (mBio03343-24-s0004.docx). Membrane-bound OXAs and its soluble variants confers similar resistance phenotypes.
Table S4 (mBio03343-24-s0005.docx). Membrane-bound OXAs are more prone to be incorporated into OMVs than soluble ones, and exert a higher protective effect in susceptible coexisting bacteria.
Movie S1 (mBio03343-24-s0006.mp4). Representative CG-MD simulation of OXA-23 with the inner leaflet of the *A. baumannii* OM.
Movie S2 (mBio03343-24-s0007.mp4). Representative CG-MD simulation of OXA-24/40 with the inner leaflet of the *A. baumannii* OM.

REFERENCES

1. Bush K, Bradford PA. 2020. Epidemiology of β-lactamase-producing pathogens. Clin Microbiol Rev 33:00047–00119. https://doi.org/10.1128/CMR.00047-19
2. Bonomo RA. 2017. β-Lactamases: a focus on current challenges. Cold Spring Harb Perspect Med 7:a025239. https://doi.org/10.1101/cshperspect.a025239
3. Naas T, Oueslati S, Bonnin RA, Dabos ML, Zavala A, Dortet L, Retailleau P, Iorga BI. 2017. Beta-lactamase database (BLDB) - structure and function. J Enzyme Inhib Med Chem 32:917–919. https://doi.org/10.1080/14756366.2017.1344235
4. Llarrull LI, Testero SA, Fisher JF, Mobashery S. 2010. The future of the β-lactams. Curr Opin Microbiol 13:551–557. https://doi.org/10.1016/j.mib.2010.09.008
5. Bush K, Jacoby GA. 2010. Updated functional classification of β-lactamases. Antimicrob Agents Chemother 54:969–976. https://doi.org/10.1128/AAC.01009-09
6. Tooke CL, Hinchliffe P, Bragginton EC, Colenso CK, Hirvonen VHA, Takebayashi Y, Spencer J. 2019. β-Lactamases and β-Lactamase Inhibitors in the 21st century. J Mol Biol 431:3472–3500. https://doi.org/10.1016/j.jmb.2019.04.002
7. Philippon A, Dusart J, Joris B, Frère JM. 1998. The diversity, structure and regulation of β-lactamases. Cell Mol Life Sci 54:341–346. https://doi.org/10.1007/s000180050161
8. Bahr G, González LJ, Vila AJ. 2021. Metallo-β-lactamases in the age of multidrug resistance: from structure and mechanism to evolution, dissemination, and inhibitor design. Chem Rev 121:7957–8094. https://doi.org/10.1021/acs.chemrev.1c00138
9. Bonomo RA, Burd EM, Conly J, Limbago BM, Poirel L, Segre JA, Westblade LF. 2018. Carbapenemase-producing organisms: a global scourge. Clin Infect Dis 66:1290–1297. https://doi.org/10.1093/cid/cix893
10. McKenna M. 2013. The last resort: health officials are watching in horror as bacteria become resistant to powerful *carbapenem* antibiotics--one of the last drugs on the shelf. Nature New Biol 499:394–397. https://doi.org/10.1038/499394a
11. Leonard DA, Bonomo RA, Powers RA. 2013. Class D β-lactamases: a reappraisal after five decades. Acc Chem Res 46:2407–2415. https://doi.org/10.1021/ar300327a
12. Yoon E-J, Jeong SH. 2021. Class D β-lactamases. J Antimicrob Chemother 76:836–864. https://doi.org/10.1093/jac/dkaa513
13. Pradel N, Delmas J, Wu LF, Santini CL, Bonnet R. 2009. Sec-and Tat-dependent translocation of β-lactamases across the *Escherichia coli* inner membrane. Antimicrob Agents Chemother 53:242–248. https://doi.org/10.1128/AAC.00642-08
14. Denks K, Vogt A, Sachelaru I, Petriman N-A, Kudva R, Koch H-G. 2014. The Sec translocon mediated protein transport in prokaryotes and eukaryotes. Mol Membr Biol 31:58–84. https://doi.org/10.3109/09687688.2014.907455
15. Morán-Barrio J, Limansky AS, Viale AM. 2009. Secretion of *Escherichia coli* metallo-beta-lactamase in *Escherichia coli* depends strictly on the cooperation between the cytoplasmic DnaK chaperone system and the Sec machinery: completion of folding and Zn(II) ion acquisition occur in the bacterial periplasm. Antimicrob Agents Chemother 53:2908–2917. https://doi.org/10.1128/AAC.01637-08
16. Kaderabkova N, Bharathwaj M, Furniss RCD, Gonzalez D, Palmer T, Mavridou DAI. 2022. The biogenesis of β-lactamase enzymes. Microbiology (Reading, Engl) 168:001217. https://doi.org/10.1099/mic.0.001217
17. Bootsma HJ, van Dijk H, Verhoef J, Fleer A, Mooi FR. 1996. Molecular characterization of the Moraxella (Branhamella) catarrhalis BRO beta-lactamase. Antimicrob Agents Chemother 40:966–972. https://doi.org/10.1128/AAC.40.4.966
18. Randall LB, Dobos K, Papp-Wallace KM, Bonomo RA, Schweizer HP. 2016. Membrane-bound PenA β-lactamase of *Burkholderia pseudomallei*. Antimicrob Agents Chemother 60:1509–1514. https://doi.org/10.1128/AAC.02444-15
19. González LJ, Bahr G, Nakashige TG, Nolan EM, Bonomo RA, Vila AJ. 2016. Membrane anchoring stabilizes and favors secretion of New Delhi metallo-β-lactamase. Nat Chem Biol 12:516–522. https://doi.org/10.1038/nchembio.2083
20. Martínez MMB, Bonomo RA, Vila AJ, Maffía PC, González LJ. 2021. On the offensive: the role of outer membrane vesicles in the successful dissemination of New Delhi metallo-β-lactamase (NDM-1). MBio 12:e0183621. https://doi.org/10.1128/mBio.01836-21
21. López C, Delmonti J, Bonomo RA, Vila AJ. 2022. Deciphering the evolution of metallo-β-lactamases: a journey from the test tube to the

bacterial periplasm. J Biol Chem 298:101665. https://doi.org/10.1016/j.jbc.2022.101665
22. Auclair SM, Bhanu MK, Kendall DA. 2012. Signal peptidase I: cleaving the way to mature proteins. Protein Sci 21:13–25. https://doi.org/10.1002/pro.757
23. Vogeley L, El Arnaout T, Bailey J, Stansfeld PJ, Boland C, Caffrey M. 2016. Structural basis of lipoprotein signal peptidase II action and inhibition by the antibiotic globomycin. Science 351:876–880. https://doi.org/10.1126/science.aad3747
24. Zückert WR. 2014. Secretion of bacterial lipoproteins: through the cytoplasmic membrane, the periplasm and beyond. Biochim Biophys Acta 1843:1509–1516. https://doi.org/10.1016/j.bbamcr.2014.04.022
25. Narita S, Matsuyama S, Tokuda H. 2004. Lipoprotein trafficking in *Escherichia coli*. Arch Microbiol 182:1–6. https://doi.org/10.1007/s00203-004-0682-4
26. Babu MM, Priya ML, Selvan AT, Madera M, Gough J, Aravind L, Sankaran K. 2006. A database of bacterial lipoproteins (DOLOP) with functional assignments to predicted lipoproteins. J Bacteriol 188:2761–2773. https://doi.org/10.1128/JB.188.8.2761-2773.2006
27. Okuda S, Tokuda H. 2011. Lipoprotein sorting in bacteria. Annu Rev Microbiol 65:239–259. https://doi.org/10.1146/annurev-micro-090110-102859
28. Tanaka S, Narita S, Tokuda H. 2007. Characterization of the *Pseudomonas aeruginosa* lol system as a lipoprotein sorting mechanism. J Biol Chem 282:13379–13384. https://doi.org/10.1074/jbc.M611840200
29. Bei W, Luo Q, Shi H, Zhou H, Zhou M, Zhang X, Huang Y. 2022. Cryo-EM structures of *Escherichia coli* LolCDE reveal the molecular mechanism of bacterial lipoprotein sorting in *Escherichia coli*. PLoS Biol 20:e3001823. https://doi.org/10.1371/journal.pbio.3001823
30. Toyofuku M, Nomura N, Eberl L. 2019. Types and origins of bacterial membrane vesicles. Nat Rev Microbiol 17:13–24. https://doi.org/10.1038/s41579-018-0112-2
31. McBroom AJ, Kuehn MJ. 2005. Outer membrane vesicles. EcoSal Plus 1:4. https://doi.org/10.1128/ecosal.2.2.4
32. McMillan HM, Kuehn MJ. 2021. The extracellular vesicle generation paradox: a bacterial point of view. EMBO J 40:e108174. https://doi.org/10.15252/embj.2021108174
33. Brown L, Wolf JM, Prados-Rosales R, Casadevall A. 2015. Through the wall: extracellular vesicles in Gram-positive bacteria, mycobacteria and fungi. Nat Rev Microbiol 13:620–630. https://doi.org/10.1038/nrmicro3480
34. Chatterjee S, Mondal A, Mitra S, Basu S. 2017. *Acinetobacter baumannii* transfers the blaNDM-1 gene via outer membrane vesicles. J Antimicrob Chemother 72:2201–2207. https://doi.org/10.1093/jac/dkx131
35. Tang B, Yang A, Liu P, Wang Z, Jian Z, Chen X, Yan Q, Liang X, Liu W. 2023. Outer membrane vesicles transmitting bla NDM-1 mediate the emergence of *Klebsiella pneumoniae*. Antimicrob Agents Chemother 67:e01444-22. https://doi.org/10.1128/aac.01444-22
36. Prunotto A, Bahr G, González LJ, Vila AJ, Dal Peraro M. 2020. Molecular bases of the membrane association mechanism potentiating antibiotic resistance by New Delhi metallo-β-lactamase 1. ACS Infect Dis 6:2719–2731. https://doi.org/10.1021/acsinfecdis.0c00341
37. López C, Prunotto A, Bahr G, Bonomo RA, González LJ, Dal Peraro M, Vila AJ. 2021. Specific protein-membrane interactions promote packaging of metallo-β-lactamases into outer membrane vesicles. Antimicrob Agents Chemother 65:e0050721. https://doi.org/10.1128/AAC.00507-21
38. Teufel F, Almagro Armenteros JJ, Johansen AR, Gíslason MH, Pihl SI, Tsirigos KD, Winther O, Brunak S, von Heijne G, Nielsen H. 2022. SignalP 6.0 predicts all five types of signal peptides using protein language models. Nat Biotechnol 40:1023–1025. https://doi.org/10.1038/s41587-021-01156-3
39. Hussain M, Pastor FI, Lampen JO. 1987. Cloning and sequencing of the blaZ gene encoding beta-lactamase III, a lipoprotein of *Bacillus cereus* 569/H. J Bacteriol 169:579–586. https://doi.org/10.1128/jb.169.2.579-586.1987
40. Souza PCT, Alessandri R, Barnoud J, Thallmair S, Faustino I, Grünewald F, Patmanidis I, Abdizadeh H, Bruininks BMH, Wassenaar TA, et al. 2021. Martini 3: a general purpose force field for coarse-grained molecular dynamics. Nat Methods 18:382–388. https://doi.org/10.1038/s41592-021-01098-3
41. Abraham EP, Chain E. 1940. An enzyme from bacteria able to destroy penicillin. Nat New Biol 146:837–837. https://doi.org/10.1038/146837a0
42. Hede K. 2014. Antibiotic resistance: an infectious arms race. Nat New Biol 509:S2–3. https://doi.org/10.1038/509S2a
43. Lisa M-N, Palacios AR, Aitha M, González MM, Moreno DM, Crowder MW, Bonomo RA, Spencer J, Tierney DL, Llarrull LI, Vila AJ. 2017. A general reaction mechanism for carbapenem hydrolysis by mononuclear and binuclear metallo-β-lactamases. Nat Commun 8:538. https://doi.org/10.1038/s41467-017-00601-9
44. Golemi D, Maveyraud L, Vakulenko S, Samama J-P, Mobashery S. 2001. Critical involvement of a carbamylated lysine in catalytic function of class D β-lactamases. Proc Natl Acad Sci U S A 98:14280–14285. https://doi.org/10.1073/pnas.241442898
45. Zhou Q, Catalán P, Bell H, Baumann P, Cooke R, Evans R, Yang J, Zhang Z, Zappalà D, Zhang Y, Blackburn GM, He Y, Jin Y. 2023. An ion-pair induced intermediate complex captured in class D carbapenemase reveals chloride ion as a janus effector modulating activity. ACS Cent Sci 9:2339–2349. https://doi.org/10.1021/acscentsci.3c00609
46. López C, Ayala JA, Bonomo RA, González LJ, Vila AJ. 2019. Protein determinants of dissemination and host specificity of metallo-*β-lactamases*
47. Bahr G, Vitor-Horen L, Bethel CR, Bonomo RA, González LJ, Vila AJ. 2018. Clinical evolution of New Delhi metallo-β-lactamase (NDM) optimizes resistance under Zn (II) deprivation. Antimicrob Agents Chemother 62:e01849-17. https://doi.org/10.1128/AAC.01849-17
48. Wu X, Chavez JD, Schweppe DK, Zheng C, Weisbrod CR, Eng JK, Murali A, Lee SA, Ramage E, Gallagher LA, Kulasekara HD, Edrozo ME, Kamischke CN, Brittnacher MJ, Miller SI, Singh PK, Manoil C, Bruce JE. 2016. *In vivo* protein interaction network analysis reveals **Acinetobacter baumannii** strain AB5075. Nat Commun 7:13414. https://doi.org/10.1038/ncomms13414
49. Yun SH, Park EC, Lee S-Y, Lee H, Choi C-W, Yi Y-S, Ro H-J, Lee JC, Jun S, Kim H-Y, Kim G-H, Kim SI. 2018. Antibiotic treatment modulates protein components of cytotoxic outer membrane vesicles of multidrug-resistant clinical strain, *Acinetobacter baumannii* DU202. Clin Proteomics 15:28. https://doi.org/10.1186/s12014-018-9204-2
50. Liao Y-T, Kuo S-C, Chiang M-H, Lee Y-T, Sung W-C, Chen Y-H, Chen T-L, Fung C-P. 2015. *Acinetobacter baumannii* extracellular OXA-58 is primarily and selectively released via outer membrane vesicles after Sec-dependent periplasmic translocation. Antimicrob Agents Chemother 59:7346–7354. https://doi.org/10.1128/AAC.01343-15
51. Colquhoun JM, Farokhyfar M, Hutcheson AR, Anderson A, Bethel CR, Bonomo RA, Clarke AJ, Rather PN. 2021. OXA-23 β-lactamase overexpression in *Acinetobacter baumannii* drives physiological changes resulting in new genetic vulnerabilities. MBio 12:e0313721. https://doi.org/10.1128/mBio.03137-21
52. Marchaim D, Perez F, Lee J, Bheemreddy S, Hujer AM, Rudin S, Hayakawa K, Lephart PR, Blunden C, Shango M, Campbell ML, Varkey J, Manickam P, Patel D, Pogue JM, Chopra T, Martin ET, Dhar S, Bonomo RA, Kaye KS. 2012. *Enterobacteriaceae Acinetobacter baumannii Pseudomonas aeruginosa* "Swimming in resistance": co-colonization with carbapenem-resistant *Enterobacteriaceae* and *Acinetobacter baumannii* or *Pseudomonas aeruginosa*. Am J Infect Control 40:830–835. https://doi.org/10.1016/j.ajic.2011.10.013
53. Maragakis LL, Tucker MG, Miller RG, Carroll KC, Perl TM. 2008. Incidence and prevalence of multidrug-resistant *Acinetobacter* using targeted active surveillance cultures. JAMA 299:2513–2514. https://doi.org/10.1001/jama.299.21.2513
54. Mammina C, Bonura C, Vivoli AR, Di Bernardo F, Sodano C, Saporito MA, Verde MS, Saporito L, Cracchiolo AN, Fabbri PG, Tetamo R, Palma DM. 2013. Co-colonization with *Klebsiella pneumoniae* and *Acinetobacter baumannii* in intensive care unit patients. Scand J Infect Dis 45:629–634. https://doi.org/10.3109/00365548.2013.782614
55. Semenec L, Cain AK, Dawson CJ, Liu Q, Dinh H, Lott H, Penesyan A, Maharjan R, Short FL, Hassan KA, Paulsen IT. 2023. Cross-protection and cross-feeding between *Klebsiella pneumoniae* and *Acinetobacter baumannii* promotes their co-existence. Nat Commun 14:702. https://doi.org/10.1038/s41467-023-36252-2
56. Rumbo C, Fernández-Moreira E, Merino M, Poza M, Mendez JA, Soares NC, Mosquera A, Chaves F, Bou G. 2011. Horizontal transfer of the OXA-24 carbapenemase gene via outer membrane vesicles: a new

mechanism of dissemination of carbapenem resistance genes in *Acinetobacter baumannii*. Antimicrob Agents Chemother 55:3084–3090. https://doi.org/10.1128/AAC.00929-10
57. Cock PJA, Antao T, Chang JT, Chapman BA, Cox CJ, Dalke A, Friedberg I, Hamelryck T, Kauff F, Wilczynski B, de Hoon MJL. 2009. Biopython: freely available python tools for computational molecular biology and bioinformatics. Bioinformatics 25:1422–1423. https://doi.org/10.1093/bioinformatics/btp163
58. Varadi M, Anyango S, Deshpande M, Nair S, Natassia C, Yordanova G, Yuan D, Stroe O, Wood G, Laydon A, et al. 2022. AlphaFold protein structure database: massively expanding the structural coverage of protein-sequence space with high-accuracy models. Nucleic Acids Res 50:D439–D444. https://doi.org/10.1093/nar/gkab1061
59. Ruch P, Teodoro D, ConsortiumU. 2021. Uniprot
60. Berman HM, Westbrook J, Feng Z, Gilliland G, Bhat TN, Weissig H, Shindyalov IN, Bourne PE. 2000. The protein data bank. Nucleic Acids Res 28:235–242. https://doi.org/10.1093/nar/28.1.235
61. Kroon PC, Grünewald F, Barnoud J, Tilburg M, Souza PC, Wassenaar TA, Marrink S-J. 2022. Martinize2 and vermouth: unified framework for topology generation. arXiv. https://doi.org/10.7554/eLife.90627.1
62. Rao S, Bates GT, Matthews CR, Newport TD, Vickery ON, Stansfeld PJ. 2020. Characterizing membrane association and periplasmic transfer of bacterial lipoproteins through molecular dynamics simulations. Structure 28:475–487. https://doi.org/10.1016/j.str.2020.01.012
63. Wassenaar TA, Ingólfsson HI, Böckmann RA, Tieleman DP, Marrink SJ. 2015. Computational lipidomics with insane: a versatile tool for generating custom membranes for molecular simulations. J Chem Theory Comput 11:2144–2155. https://doi.org/10.1021/acs.jctc.5b00209
64. Jiang X, Yang K, Yuan B, Han M, Zhu Y, Roberts KD, Patil NA, Li J, Gong B, Hancock REW, Velkov T, Schreiber F, Wang L, Li J. 2020. Molecular dynamics simulations informed by membrane lipidomics reveal the structure–interaction relationship of polymyxins with the lipid a-based outer membrane of *Acinetobacter baumannii*. J Antimicrob Chemother 75:3534–3543. https://doi.org/10.1093/jac/dkaa376
65. Corey RA, Song W, Duncan AL, Ansell TB, Sansom MSP, Stansfeld PJ. 2021. Identification and assessment of cardiolipin interactions with *E. coli* inner membrane proteins. Sci Adv 7:eabh2217. https://doi.org/10.1126/sciadv.abh2217
66. Abraham MJ, Murtola T, Schulz R, Páll S, Smith JC, Hess B, Lindahl E. 2015. GROMACS: high performance molecular simulations through multi-level parallelism from laptops to supercomputers. SoftwareX 1–2:19–25. https://doi.org/10.1016/j.softx.2015.06.001
67. Tironi IG, Sperb R, Smith PE, van Gunsteren WF. 1995. A generalized reaction field method for molecular dynamics simulations. J Chem Phys 102:5451–5459. https://doi.org/10.1063/1.469273
68. Jo S, Kim T, Iyer VG, Im W. 2008. CHARMM‐GUI: a web‐based graphical user interface for CHARMM. J Comput Chem 29:1859–1865. https://doi.org/10.1002/jcc.20945
69. Bussi G, Donadio D, Parrinello M. 2007. Canonical sampling through velocity rescaling. J Chem Phys 126:014101. https://doi.org/10.1063/1.2408420
70. Parrinello M, Rahman A. 1980. Crystal structure and pair potentials: a molecular-dynamics study. Phys Rev Lett 45:1196–1199. https://doi.org/10.1103/PhysRevLett.45.1196
71. Sejdiu BI, Tieleman DP. 2021. ProLint: a web-based framework for the automated data analysis and visualization of lipid-protein interactions. Nucleic Acids Res 49:W544–W550. https://doi.org/10.1093/nar/gkab409
72. Humphrey W, Dalke A, Schulten K. 1996. VMD: visual molecular dynamics. J Mol Graph 14:33–38, https://doi.org/10.1016/0263-7855(96)00018-5
73. Goddard TD, Huang CC, Meng EC, Pettersen EF, Couch GS, Morris JH, Ferrin TE. 2018. UCSF ChimeraX: meeting modern challenges in visualization and analysis. Protein Sci 27:14–25. https://doi.org/10.1002/pro.3235
74. Petiti M, Houot L, Duché D. 2017. Cell fractionation. Methods Mol Biol 1615:59–64. https://doi.org/10.1007/978-1-4939-7033-9_3
75. Istvan L. GelAnalyzer 23.1.1. www.gelanalyzer.com.
76. Schwechheimer C, Kulp A, Kuehn MJ. 2014. Modulation of bacterial outer membrane vesicle production by envelope structure and content. BMC Microbiol 14:324. https://doi.org/10.1186/s12866-014-0324-1